Non-steroidal anti-inflammatory drugs have anti-amyloidogenic effects for Alzheimer's β-amyloid fibrils in vitro

メタデータ	言語: eng
	出版者:
	公開日: 2017-10-05
	キーワード (Ja):
	キーワード (En):
	作成者:
	メールアドレス:
	所属:
URL	http://hdl.handle.net/2297/7405

Non-steroidal anti-inflammatory drugs have anti-amyloidogenic effects for Alzheimer's ß-amyloid fibrils in vitro

Running title: Anti-amyloidogenic effects of NSAIDs

Authors. Mie Hirohata [a, b], Kenjiro Ono [a], Hironobu Naiki [b, c], Masahito Yamada [a, *]

[a] *Department of Neurology and Neurobiology of Aging, Kanazawa University Graduate School of Medical Science, Kanazawa 920-8640, Japan*

[b] *Division of Molecular Pathology, Department of Pathological Sciences, Faculty of Medical Sciences, University of Fukui, Fukui 910-1193, Japan*

[c] *CREST, Japan Science and Technology Agency, Saitama 332-0012, Japan*

Keywords: Alzheimer's disease; ß-amyloid fibrils; electron microscopy; non-steroidal anti-inflammatory drugs; thioflavin T.

* **Corresponding author.** Masahito Yamada,

Department of Neurology and Neurobiology of Aging, Kanazawa University Graduate School of Medical Science, Kanazawa 920-8640, Japan. Tel.: +81-76-265-2290; fax: +81-76-234-4253.

E-mail address: m-yamada@med.kanazawa-u.ac.jp

Abstract

The pathogenesis of Alzheimer's disease (AD) is characterized by cerebral deposits of amyloid ß-peptides (Aß) and neurofibrillary tangles which are surrounded by inflammatory cells. Long-term uses of non-steroidal anti-inflammatory drugs (NSAIDs) reduce the risk of developing AD and delay the onset of the disease. In the present study, we used fluorescence spectroscopy with thioflavin T and electron microscopy to examine the effects of NSAIDs such as ibuprofen, aspirin, meclofenamic acid sodium salt, diclofenac sodium salt, ketoprofen, flurbiprofen, naproxen, sulindac sulfide and indomethacin on the formation, extension, and destabilization of ß-amyloid fibrils (fAß) at pH 7.5 at 37˚C in vitro. All examined NSAIDs dose-dependently inhibited formation of fAß from fresh Aß(1-40) and Aß(1-42), as well as their extension. Moreover, these NSAIDs dose-dependently destabilized preformed fAßs. The overall activity of the molecules examined was in the following order: ibuprofen ≈ sulindac sulfide ≥ meclofenamic acid sodium salt > aspirin ≈ ketoprofen ≥ flurbiprofen ≈ diclofenac sodium salt > naproxen ≈ indomethacin. Although the mechanisms by which these NSAIDs inhibit fAß formation from Aß, and destabilize preformed fAß in vitro are still unclear, NSAIDs may be promising for the prevention and treatment of AD.

Keywords: Alzheimer's disease; ß-amyloid fibrils; electron microscopy; non-steroidal anti-inflammatory drugs; thioflavin T.

1. Introduction

In the pathogenesis of Alzheimer's disease (AD), the abundance of intraneural neurofibrillary tangles and the extracellular deposition of the amyloid ß-peptide (Aß) as amyloid plaques and vascular amyloid are seminal events (Selkoe, 2001). The aggregation of Aß and ß-sheet formation are considered to be critical events that render these peptides neurotoxic (Pike et al., 1995). The presence of chronic neuroinflammation also contributes to the protracted degenerative course of AD (McGeer and McGeer, 1995), and it is also common to other neurodegenerative disorders, such as Parkinson's disease and Creutzfelt-Jacob disease (Eikelenboom et al., 2002; Gao et al., 2003). A chronic inflammatory response characterized by activated microglia, reactive astrocytes, complement factors, and increased inflammatory cytokine expression associated with Aß deposits has been described in the brain of AD patients (Rogers et al., 1996). A number of epidemiological studies have demonstrated a reduced risk for AD in population with long-term use of non-steroidal anti-inflammatory drugs (NSAIDs) (McGeer et al., 1996; in t'Veld et al., 1998; Akiyama et al., 2000; in t'Veld et al., 2001).

These epidemiological findings have been supported by experimental studies. First, chronic ibuprofen (Ibu) treatment significantly diminished amyloid deposition (Lim et al., 2000), and improved behavioral impairment in the APPsw transgenic mouse (Tg2576) (Lim et al., 2001). Second, a subset of NSAIDs such as Ibu, sulindac sulfide (SSide), indomethacin (Ind) (Weggen et al., 2001) and flurbiprofen (Flu) (Eriksen et al., 2003) selectively decreased the secretion of Aß(1-42) from cultured cells independently of cyclooxygenase (COX) activity and lowered the amount of soluble Aß(1-42) in the brains of Tg2576 mouse. Third, SSide and enantiomers of Flu have been reported to target γ-secretase and preferentially reduce Aß(1-42) generation (Takahashi et al., 2003; Eriksen et al., 2003).

These data suggest that some of the NSAIDs may affect the pathogenetic process of AD directly. However, except the preliminary study where Thomas et al. (2001) used the non-physiological short peptide Aß(25-35), the effects of NSAIDs on the formation and destabilization of Alzheimer's ß-amyloid fibrils (fAß) in vitro have not been studied in detail.

Using a nucleation-dependent polymerization model explaining the mechanism of fAß formation in vitro (Jarrnet and Lansbury, 1993; Naiki and Gejyo, 1999), we previously found that nordihydroguaiaretic acid (NDGA) and rifampicin (Rif) inhibit fAß formation from Aß and fAß extention dose-dependently (Naiki et al., 1998). Moreover, we reported that they also destabilize fAß(1-40) and fAß(1-42) in a concentration-dependent manner within a few hours at pH 7.5 at 37˚C, based on fluorescence spectroscopic analysis with thioflavin T (ThT) and electron microscopic studies (Ono et al., 2002b).

Here, we examined the effects of the major NSAIDs on the formation, extension, and destabilization of fAß(1-40) and fAß(1-42) at pH 7.5 and 37˚C in vitro, using fluorescence spectroscopy with ThT and electron microscopy.

2. Methods

2.1. Preparation of Aß and fAß solutions

Aß(1-40) (trifluoroacetate salt, lot number 540111 and 530108, Peptide Institute Inc., Osaka, Japan) and Aß(1-42) (trifluoroacetate salt, lot number 540127 and 530914, Peptide Institute Inc., Osaka, Japan)

were dissolved by brief vortexing in 0.02% ammonia solution at a concentration of 500 µM (2.2 mg/mL) and 250 µM, respectively, in a 4˚C room and stored at -80˚C before assaying (fresh Aß(1-40) and Aß(1-42) solutions). fAß(1-40) and fAß(1-42) were formed from the fresh Aß(1-40) and Aß(1-42) solutions, respectively, sonicated, and stored at 4˚C as described elsewhere (Hasegawa et al., 1999).

Fresh, non-aggregated fAß(1-40) and fAß(1-42) were obtained by extending sonicated fAß(1-40) or fAß(1-42) with fresh Aß(1-40) or Aß(1-42) solutions, respectively, just before the destabilization reaction (Ono et al., 2002a; 2002b) . The reaction mixture was 600 µL and contained 10 µg/mL (2.3 µM) fAß(1-40) or fAß(1-42), 50 µM Aß(1-40) or Aß(1-42), 50 mM phosphate buffer, pH 7.5, and 100 mM NaCl. After incubation at 37˚C for 3-6 h under non-agitated conditions, the extension reaction proceed to equilibrium as measured by the fluorescence of ThT. In the following experiment, the concentration of fAß(1-40) and fAß(1-42) in the final reaction mixture was regarded as 50 µM.

2.2. Fluorescence spectroscopy, electron microscopy, and polarized light microscopy.

A fluorescence spectroscopic study was performed as described by Naiki and Nakakuki (1996) on a Hitachi F-2500 fluorescence spectrophotometer (Tokyo, Japan). Optimum fluorescence measurement of fAß(1-40) and fAß(1-42) were obtained at the excitation and emission wavelengths of 445 and 490 nm, respectively, with the reaction mixture containing 5 µM ThT (Wako Pure Chemical Industries Ltd, Osaka, Japan) and 50 mM of glycine-NaOH buffer, pH 8.5. An electron microscopic study and polarized light microscopic study of the reaction mixtures were performed as described elsewhere

(Hasegawa et al., 1999).

2.3. Polymerization assay

Polymerization of Aß with or without fAß added as seeds was assayed as described elsewhere (Naiki et al., 1998). The reaction mixture contained 50 µM Aß(1-40), or 25 or 50 µM Aß(1-42), 0 or 10 µg/mL fAß(1-40) or fAß(1-42), 0, 0.01, 0.1, 1, 10, or 50 µM NSAIDs (Ibu, aspirin (Asp), meclofenamic acid sodium salt (Mec), diclofenac sodium salt (Dic), ketoprofen (Ket), Flu, naproxen (Nap), SSide, Ind), NDGA, Rif, or nicotine (Sigma Chemical Co., St. Louis, MO, USA), 1% dimethyl sulfoxide (DMSO) (Nacakai Tesque, Inc., Kyoto, Japan), 50 mM phosphate buffer, pH 7.5, and 100 mM NaCl. NSAIDs dissolved in DMSO at concentrations of 1, 10, 100 µM, 1 mM and 5 mM, were added to the reaction mixture to make the final concentration 0.01, 0.1, 1, 10 µM and 50 µM, respectively.

Aliquots (30 µL) of the mixture were put into oil-free PCR tubes (size: 0.5 mL, code number: 9046; Takara Shuzo Co. Ltd, Otsu, Japan). The reaction tubes were then put into a DNA thermal cycler (PJ480; Perkin Elmer Cetus, Emeryville, CA, USA). The plate temperature was elevated at maximal speed, starting at 4˚C, to 37˚C. Incubation times ranged between 0 and 8 days (as indicated in each figure), and the reaction was stopped by placing the tubes on ice. The reaction tubes were not agitated during the reaction. From each reaction tube, triplicate 5 µL aliquots were removed, then subjected to fluorescence spectroscopy and the mean of each triplicate determined. In the ThT solution, the concentration of NSAIDs examined in this study was diluted up to 1/200 of that in the reaction mixture.

We confirmed that these compounds did not quench ThT fluorescence at the diluted concentration (data not shown).

2.4. Destabilization assay

Destabilization of fAß was assayed as described elsewhere (Ono et al., 2002b). Briefly, the reaction mixture contained 25 µM fresh fAß(1-40) or fAß(1-42), 0, 0.01, 0.1, 1, 10 or 50 µM NSAIDs, NDGA, Rif, or nicotine, 1% DMSO, 50 mM phosphate buffer, pH 7.5, 100 mM NaCl, and 1% (wt/vol) polyvinyl alcohol (Wako Pure Chemical Industries Ltd) to avoid the aggregation of fAß and the adsorption of fAß onto the inner wall of the tube during the reaction.

After being mixed by pipetting, triplicate 5 µL aliquots were subjected to fluorescence spectroscopy and 30 µL aliquots were put into oil-free PCR tubes (Takara Shuzo Co. Ltd, Otsu, Japan). The reaction tubes were then transferred into a DNA thermal cycler (Perkin Elmer Cetus, Emeryville, California). Starting at 4˚C, the plate temperature was elevated at maximal speed to 37˚C. Incubation times ranged from 0 to 24 h (as indicated in each figure), and the reaction was stopped by placing the tubes on ice. The reaction tubes were not agitated during the reaction. From each reaction tube, 5 µL aliquots in triplicate were subjected to fluorescence spectroscopy and the mean of the three measurements was determined. ThT fluorescence did not change significantly when fAß were incubated with 0-50 µM of NSAIDs at either 4˚C or 37˚C for 1 min, then subjected to ThT assay, indicating that these compounds did not compete with ThT for fAß (data not shown).

2.5. Other analytical procedures

Protein concentrations of Aßs and fAßs in the reaction mixtures were determined by the method of Bradford (1976) with a protein assay kit (Bio-Rad Laboratories, Inc., Hercules, CA). The Aß(1-40) solution quantified by amino acid analysis was used as the standard. The linear least squares fit and one-way analysis of variance, post-hoc test by Scheffe were used for statistical analysis.

3. Results

3.1. Effect of NSAIDs on the kinetics of fAß polymerization

As shown in Fig. 1A-D, the fluorescence of ThT followed a characteristic sigmoidal curve when fresh Aß(1-40) or Aß(1-42) was incubated at 37°C. This curve is consistent with a nucleation-dependent polymerization model (Jarrett and Lansbury, 1993; Naiki and Gejyo, 1999). Fresh fAß(1-40) assumed a non-branched, helical filament structure of approximately 10 nm width and exhibited a helical periodicity of approximately 220 nm. In the fresh fAß(1-42) solution, two types of filaments of approximately 8 and 12 nm width were observed. Although the Aß batches used here were different from those in our previous experiments, these morphologies of fAßs were similar to those reported previously (Naiki and Nakakuki, 1996; Naiki et al., 1998). Both fAß(1-40) and fAß(1-42) stained with Congo red showed typical orange-green birefringence under polarized light. The final equilibrium level of Aß(1-40) or Aß(1-42) was lowered dose-dependently by incubation with

10 and 50 μM Ibu, Ket or Nap (Fig. 1A-D). Other NSAIDs (Asp, Mec, Dic, Flu, SSide and Ind) also significantly inhibited the polymerization of Aß(1-40) and Aß(1-42) (Fig. 6A, B).

As shown in Fig. 2A-D, the fluorescence increased hyperbolically without a lag phase and proceeded to equilibrium much more rapidly by incubation of fresh Aß(1-40) or Aß(1-42) with fAß(1-40) or fAß(1-42), respectively, at 37˚C, than that without seeds (compare Fig. 1A, B, and 2A, B). This curve is consistent with a first-order kinetic model (Naiki and Nakakuki, 1996). The final equilibrium level was dose-dependently decreased by incubation of Aß(1-40) or Aß(1-42) with fAß(1-40) or Aß(1-42), respectively, with 10 or 50 μM Ibu, Ket or Nap (Fig. 2A-D). Other NSAIDs (Asp, Mec, Dic, Flu, SSide and Ind) also significantly inhibited the extension of fAß(1-40) and fAß(1-42) (data not shown).

As shown in Fig. 2E, at a constant fAß(1-40) concentration, a good linearity was observed between the Aß(1-40) concentration and the initial rate of fAß(1-40) extension both in the presence and absence of Ibu. This linearity is again consistent with a first-order kinetic model and indicates that at each Aß(1-40) concentration, the net rate of fAß(1-40) extension is the sum of the rates of polymerization and depolymerization (Naiki and Nakakuki, 1996; Hasegawa et al., 2002). In the presence of 10 μM Ibu, the slope of the straight line decreased to about 36%.

As shown in Fig. 3B, clear fibril extension was observed by electron microscopy when fresh Aß(1-40) was incubated with fAß(1-40) at 37˚C. However, 50 μM Ibu completely inhibited the extension of sonicated fAß(1-40) (Fig. 3A, C). Ibu inhibited the extension of fAß(1-42) and other NSAIDs (Asp, Mec, Dic, Ket, Flu, Nap, SSide and Ind) also inhibited the extension of fAß(1-40) and fAß(1-42) (data not shown).

3.2. Effect of NSAIDs on the kinetics of fAß destabilization

As shown in Fig. 4A-D, the fluorescence of ThT was almost unchanged during the incubation of fresh fAß(1-40) or fAß(1-42) at 37˚C without additional molecules. On the other hand, the ThT fluorescence decreased immediately after addition of NSAIDs to the reaction mixture. As shown in Fig. 4A-D, the ThT fluorescence of fAß(1-40) and fAß(1-42) decreased immediately after addition of Ibu, Ket, Nap, in a concentration-dependent manner. Other NSAIDs (Asp, Mec, Dic, Flu, SSide and Ind) also significantly destabilized fAß(1-40) and fAß(1-42) (Fig. 6C, D).

After incubation of 25 µM fresh fAß(1-40) with 50 µM Ibu for 1 h, many short, sheared fibrils were observed (Fig. 5B). At 6 h, the number of fibrils was markedly decreased, and small amorphous aggregates were occasionally observed (Fig. 5C). Ibu destabilized fresh fAß(1-42) and other NSAIDs (Asp, Mec, Dic, Ket, Flu, Nap, SSide and Ind) also destabilized preformed fAß(1-40) and fAß(1-42) (data not shown).

As shown in Fig. 6, statistical analysis revealed a significant difference in the potency of 50 µM NSAIDs for the anti-polymerization effect (A, B) and for the fibril destabilizing effect (C, D). In both the cases of fAß(1-40) and fAß(1-42), the potency of NSAIDs for the anti-polymerization effect was similar to that for the fibril-destabilizing effect. Additionally, similar anti-polymerization and fibril-destabilizing effects were observed for both fAßs. The overall activity of the molecules examined was in the order of: Ibu $\approx$ SSide $\geq$ Mec $>$ Asp $\approx$ Ket $\geq$ Flu $\approx$ Dic $>$ Nap $\approx$ Ind. We finally compared the anti-amyloidogenic and fibril-destabilizing activity of SSide and Ibu with that of NDGA,

Rif, and nicotine (Fig. 7). Although NDGA exhibited the potent anti-amyloidogenic and fibril-destabilizing activity dose-dependently, the activity of nicotine was weak or negligible. Rif, SSide and Ibu exhibited similar dose-dependent activity.

After incubation with 50 µM Ibu for 4 h, fAß(1-40) and fAß(1-42) were stained with Congo red much more weakly than fresh fAß(1-40) and fAß(1-42), but they all showed orange-green birefringence under polarized light. This means that a significant amount of intact fAß(1-40) and fAß(1-42) still remains in the mixture after the reaction, as shown in Fig. 5C. No proteins were detected by the Bradford assay in the supernatant after centrifugation at 4˚C for 2 h at 1.6×10^4 g. This implies that although Ibu could destabilize fAß(1-40) and fAß(1-42) to visible aggregates (Fig. 5C), they could not depolymerize fAß(1-40) and fAß(1-42) to monomers or oligomers of Aß(1-40) and Aß(1-42). When fresh 50 µM Aß(1-40) or Aß(1-42) was incubated with 10 µg/mL of the pellet at 37˚C, no increase in the fluorescence was observed for 6 h. This implies that destabilized fAß(1-40) and fAß(1-42) could not function as seeds.

4. Discussion

In this study, we demonstrated that various NSAIDs dose-dependently inhibited formation of fAß from fresh Aß(1-40) and Aß(1-42), as well as their extension in vitro. Moreover, these NSAIDs dose-dependently destabilized preformed fAßs.

Thomas et al. (2001) suggested that the anti-aggregation effect of NSAIDs may be due to their interaction with epitope 3-6 and/or 25-35 in Aß, which are considered crucial to Aß aggregation and

neurotoxicity. As shown in Fig. 2E, the extension of fAß(1-40) followed a first-order kinetic model even in the presence of Ibu. The net rate of fAß(1-40) extension is the sum of the rates of polymerization and depolymerization (Naiki and Nakakuki, 1996; Hasegawa et al., 2002). Thus, one possible explanation for the finding in Fig. 2E may be that Ibu bound to the ends of extending fAß(1-40) and increased the rate of depolymerization by destabilizing the conformation of Aß(1-40) which has just been incorporated into the fibril ends. Alternatively, Ibu would bind to Aß(1-40) and consequently decrease the rate of polymerization. Tomiyama et al. (1996) suggested that Rif binds to Aß by hydrophobic interactions between its lipophilic ansa chain and the hydrophobic region of Aß, thus blocking associations between Aß molecules leading to fAß formation. The anti-amyloidogenic and fibril-destabilizing activity of tetracycline (Tc), small-molecule anionic sulphonates or sulphates, melatonin, ß-sheet breaker peptides (iAß5) and nicotine may also be related to the propensity to bind to the specific sites of Aß (Kisilevsky et al. 1995; Soto et al. 1996; Pappolla et al. 1998; Forloni et al. 2001; Zeng et al. 2001). Thus, it may be reasonable to consider that NSAIDs could exhibit their anti-amyloidogenic and fibril-destabilizing effects by directly binding to Aßs and/or fAßs.

Taking into consideration the findings we obtained previously by systematic in vitro studies, we judged the overall activity of the anti-amyloidogenic molecules to be in the order of: tannic acid >> NDGA = wine-related polyphenols (myricetin, morin, quercetin) >> Rif = Tc > poly(vinylsulfonic acid, sodium salt) = 1,3-propanedisulfonic acid, disodium salt > iAß5 > nicotine (Ono et al., 2002a; 2002b; 2003; 2004a). In this study, we observed that the activity of SSide and Ibu is similar to that of Rif (Fig. 7).

Next, we considered the structure-activity relationships of NSAIDs and other anti-amyloidogenic

compounds. The antioxidant compounds with hydroxyphenyl rings are suggested to bind specifically to Aß and/or fAß, inhibit fAß formation and/or destabilize preformed fAß (Ono et al., 2002b; 2003; 2004a; 2004b; Li et al., 2004). On the other hand, the NSAIDs examined in this study have no hydroxyphenyl rings (Fig. 8). In general, these NSAIDs have an aromatic-based hydrophobic structure with some fused ring structures and methyl and/or carboxyl groups. This structure might be quite suitable for specifically binding to free Aß and subsequently inhibiting the polymerization of Aß into fAß. Alternatively, this structure might be suitable for a specific binding to fAß and subsequent destabilization of the ß-sheet rich conformation of Aß molecules in fAß. Further studies, such as nuclear magnetic resonance experiments, are essential to reveal the exact structure-activity relationships for NSAIDs and other organic compounds that exhibit anti-amyloidogenic and fibril-destabilizing effects in vitro.

Clinically, Ibu has been used in the treatment of nerve-root compression pain. Although their penetration into the cerebrospinal fluid (CSF) is 0.9-1.5 % of the plasma level, the CSF level of Ibu derivatives is the range 595-1241 ng h/ml in the patients taking oral doses of 800 mg Ibu (Bannwarth et al., 1995). This corresponds to 2884-6016 μM h of Ibu, which were higher than the concentration used in the present study. It is therefore conceivable that therapeutic doses of Ibu could provide a concentration sufficient to achieve the anti-amyloidogenic effects.

Recent epidemiological studies have revealed that long-term and/or short-term use of some NSAIDs may protect against AD (McGeer et al., 1996; in t'Veld et al., 1998; Akiyama et al., 2000; in t'Veld et al., 2001). Our study and several reports on the effects of NSAIDs may well explain this correlation. First, the major therapeutic effect of NSAIDs is believed to be due to their inhibition of

COX-1 and COX-2, leading to the suppression of prostaglandin synthesis and chronic neuroinflammation contributing to the protracted degenerative course of AD (McGeer and McGeer, 1995; Akiyama et al., 2000). Second, Weggen et al. (2001) recently suggested that a subset of NSAIDs including Ibu, SSide, Ind and *R*-Flu directly affect amyloid pathology in the brains of transgenic mouse by reducing the amount of soluble Aß(1-42) peptide levels independently of COX activity. They also suggested that NSAIDs subtly alter γ-secreatase activity without significantly perturbing other amyloid precursor protein (APP) pathways or Notch cleavage. Some NSAIDs were reported to lower Aß(1-42) levels selectively both in cultured cell and broken cell assays, suggesting that these compounds interact directly with the γ-secretase complex itself that generates Aß from human APP (Sagi et al., 2003; Eriksen et al., 2003). In addition, a subset of NSAIDs can reduce Aß(1-42) through inhibition of Rho activity, which may regulate APP processing in a cell culture (Zhou et al., 2003). Finally, as shown in this paper, NSAIDs dose-dependently inhibit fAß formation from fresh Aß and their extension, as well as destabilize preformed fAß in vitro. Thus, it may be reasonable to speculate that NSAIDs could prevent the development of AD, not only through suppressing chronic neuroinflammation and reducing the amount of soluble Aß(1-42) peptide levels, but also through directly inhibiting the deposition of fAß in the brain. In relation to the latter scenario, it may be essential to evaluate the effect of NSAIDs on the Aß oligomer formation in a future study, because the Aß oligomer has been reported to be the most neurotoxic form of all the Aß aggregates (Gong et al., 2003). Yang et al. (2005) recently reported that curcumin prevented Aß42 oligomer formation and toxicity between 0.1 and 1.0 µM, which is consistent with our EC_{50} values of curcumin for the anti-amyloidogenic and fibril-destabilizing activity (Ono et al., 2004b). Although the exact

mechanisms of anti-amyloidogenic and fibril-destabilizing activity of NSAIDs are unclear, the careful and safe use of them could contribute the prevention and therapy of AD and other kinds of human amyloidosis.

Acknowledgements

The authors thank Dr. K. Iwasa (Kanazawa University) for cooperation in the experiments. This work was supported in part by a Grant-in-Aid for Scientific Research from the Ministry of Education, Culture, Sports, Science and Technology, Japan (M.Y.), a grant for the knowledge-based Cluster Creation Project from the Ministry of Education, Culture, Sports, Science, and Technology, Japan (M.Y.), a grant for the 21st Century COE Program (on Innovative Brain Science for Development, Learning, and Memory) from the Ministry of Education, Culture, Sports, Science, and Technology, Japan (M.Y.), a grant for the Amyloidosis Research Committee from the Ministry of Health, Labour, and Welfare, Japan (M.Y., H.N.), and a Grant-in-Aid for Scientific Research on Priority Areas (C) – Advanced Brain Science Project – from the Ministry of Education, Culture, Sports, Science and Technology, Japan (H.N.).

References

Akiyama, H., Barger, S., Barnum, S., Bradt, B., Bauer, J., Cole, G.M., Cooper, N.R., Eikelenboom, P., Emmerling, M., Fiebich, B.L., Finch, C.E., Frautschy, S., Griffin, W.S., Hampel, H., Hull, M., Landreth, G., Lue, L., Mrak, R., Mackenzie, I.R., McGeer, P.L., O'Banion, M.K., Pachter, J., Pasinetti, G., Plata-Salaman, C., Rogers, J., Rydel, R., Shen, Y., Streit, W., Strohmeyer, R., Tooyoma, I., Van Muiswinkel, F.L., Veerhuis, R., Walker, D., Webster, S., Wegrzyniak, B., Wenk, G., Wyss-Coray, T., 2000. Inflammation and Alzheimer's disease. Neurobiol. Aging 21, 383-421.

Bannwarth, B., Lapicque, F., Pehourcq, F., Gillet, P., Schaeverbeke, T., Laborde, C., Dehais, J., Gaucher, A., Netter, P., 1995. Stereoselective disposition of ibuprofen enantiomers in human cerebrospinal fluid. Br. J. Clin. Pharmacol. 40, 266-269.

Bradford, M.M., 1976. A rapid and sensitive method for the quantitation of microgram quantities of protein utilizing the principle of protein-dye binding. Anal. Biochem. 72, 248-254.

Eikelenboom, P., Bate, C., Van Gool, W.A., Hoozemans, J.J., Rozemuller, J.M., Veerhuis, R., Williams, A., 2002. Neuroinflammation in Alzheimer's disease and prion disease. Glia 40, 232-239.

Eriksen, J.L., Sagi. S.A., Smith, T.E., Weggen, S., Das. P., McLendon. D.C., Ozols, V.V., Jessing, K.W., Zavitz, K.H., Koo, E.H., Golde, T.E., 2003. NSAIDs and enantiomers of flurbiprofen target γ-secretase and lower Aß42 in vivo. J. Clin. Invest. 112, 440-449.

Forloni, G., Colombo, L., Girola, L., Tagliavini, F., Salmona, M., 2001. Anti-amyloidogenic activity of tetracyclines: studies in vitro. F. E. B. S. Lett. 487, 404-407.

Gao, H.M., Liu, B., Zhang, W., Hong, J.S., 2003. Novel anti-inflammatory therapy for Parkinson's disease. Trends Pharmacol. Sci. 24, 395-401.

Gong, Y., Chang, L., Viola, K.L., Lacor, P.N., Lambert, M.P., Finch, C.E., Krafft, G.A., Klein, W.L., 2003. Alzheimer's disease-affected brain: Presence of oligomeric Aß ligands (ADDLs) suggests a molecular basis for reversible memory loss. Proc. Natl. Acad. Sci. U. S. A. 100, 10417-10422.

Hasegawa, K., Yamaguchi, I., Omata, S., Gejyo, F., Naiki, H., 1999. Interaction between Aß(1-42) and Aß(1-40) in Alzheimer's ß-amyloid fibril formation in vitro. Biochemistry 38, 15514-15521.

Hasegawa, K., Ono, K., Yamada, M., Naiki, H., 2002. Kinetic modeling and determination of reaction constants of Alzheimer's ß-amyloid fibril extension and dissociation using surface plasmon resonance. Biochemistry 41, 13489-13498.

in 't Veld, B.A., Launer, L.J., Hoes, A.W., Ott, A., Hofman, A., Breteler, M.M., Stricker, B.H., 1998. NSAIDs and incident Alzheimer's disease. The Rotterdam Study. Neurobiol. Aging 19, 607-611.

in t' Veld, B.A., Ruitenberg, A., Hofman, A., Launer, L.J., van Duijn, C.M., Stijnen, T., Breteler, M.M., Stricker, B.H., 2001. Nonsteroidal antiinflammatory drugs and the risk of Alzheimer's disease. N. Engl. J. Med. 345, 1515-1521.

Jarrett, J.T., Lansbury, P.T. Jr., 1993. Seeding "one-dimensional crystallization" of amyloid: a pathogenic mechanism in Alzheimer's disease and scrapie? Cell 73, 1055-1058.

Kisilevsky, R., Lemieux, L.J., Fraser, P.E., Kong, X., Hultin, P.G., Szarek, W.A., 1995. Arresting amyloidosis in vivo using small-molecule anionic sulphonates or sulphates: implications for Alzheimer's disease. Nat. Med. 1, 143-148.

Li, J., Zhu, M., Manning-Bog, A.B., Di Monte, D.A., Fink, A.L., 2004. Dopamine and L-dopa

disaggregate amyloid fibrils: implications for Parkinson's and Alzheimer's disease. F.A.S.E.B.J. 9, 962-964.

Lim, G.P., Yang, F., Chu, T., Chen, P., Beech, W., Teter, B., Tran, T., Ubeda, O., Ashe, K.H., Frautschy, S.A., Cole, G.M., 2000. Ibuprofen suppresses plaque pathology and inflammation in a mouse model for Alzheimer's disease. J. Neurosci. 20, 5709-5714.

Lim, G.P., Yang, F., Chu, T., Gahtan, E., Ubeda, O., Beech, W., Overmier, J.B., Hsiao-Ashec, K., Frautschy, S.A., Cole, G.M., 2001. Ibuprofen effects on Alzheimer pathology and open field activity in APPsw transgenic mice. Neurobiol. Aging 22, 983-991.

McGeer, P.L., McGeer, E.G., 1995. The inflammatory response system of brain: implications for therapy of Alzheimer and other neurodegenerative diseases. Brain. Res. Brain. Res. Rev. 21, 195-218.

McGeer, P.L., Schulzer, M., McGeer, E.G., 1996. Arthritis and anti-inflammatiry agents as possible protective factors for Alzheimer’s disease: a review of 17 epidemiologic studies. Neurology 47, 425-432.

Naiki, H., Gejyo, F., 1999. Kinetic analysis of amyloid fibril formation. Methods Enzymol. 309, 305-18.

Naiki, H., Hasegawa, K., Yamaguchi, I., Nakamura, H., Gejyo, F., Nakakuki, K., 1998. Apolipoprotein E and antioxidants have different mechanisms of inhibiting Alzheimer's ß-amyloid fibril formation in vitro. Biochemistry 37, 17882-17889.

Naiki, H., Nakakuki, K., 1996. First-order kinetic model of Alzheimer's ß-amyloid fibril extension in vitro. Lab. Invest. 74, 374-383.

Ono, K., Hasegawa, K., Yamada, M., Naiki, H., 2002a. Nicotine breaks down preformed Alzheimer's ß-amyloid fibrils in vitro. Biol. Psychiatry 52, 880-886.

Ono, K., Hasegawa, K., Yoshiike, Y., Takashima, A., Yamada, M., Naiki, H., 2002b. Nordihydroguaiaretic acid potently breaks down pre-formed Alzheimer's ß-amyloid fibrils in vitro. J. Neurochem. 81, 434-440.

Ono, K., Yoshiike, Y., Takashima, A., Hasegawa, K., Naiki, H., Yamada, M., 2003. Potent anti-amyloidogenic and fibril-destabilizing effects of polyphenols in vitro: implications for the prevention and therapeutics of Alzheimer's disease. J. Neurochem. 87, 172-181.

Ono, K., Hasegawa, K., Naiki, H., Yamada, M., 2004a. Anti-amyloidogenic activity of tannic acid and its activity to destabilize Alzheimer’s ß-amyloid fibrils in vitro. Biochim. Biophys. Acta 1690, 193-202.

Ono, K., Hasegawa, K., Naiki, H., Yamada, M., 2004b. Curcumin has potent anti-amyloidogenic effects for Alzheimer's ß-amyloid fibrils in vitro. J. Neurosci. Res. 75, 742-750.

Pappolla, M., Bozner, P., Soto, C., Shao, H., Robakis, N.K., Zagorski, M., Frangione, B., Ghiso, J., 1998. Inhibition of Alzheimer ß-fibrillogenesis by melatonin. J. Biol. Chem. 273, 7185-7188.

Pike, C.J., Walencewicz-Wasserman, A.J., Kosmoski, J., Cribbs, D.H., Glabe, C.G., Cotman, C.W., 1995. Structure-activity analyses of ß-amyloid peptides: contributions of the ß25-35 region to aggregation and neurotoxicity. J. Neurochem. 64, 253-265.

Rogers, J., Webster, S., Lue, L.F., Brachova, L., Civin, W.H., Emmerling, M., Shivers, B., Walker, D., McGeer, P., 1996. Inflammation and Alzheimer's disease pathogenesis. Neurobiol. Aging 17, 681-686.

Sagi, S.A., Weggen, S., Eriksen, J., Golde, T.E., Koo, E.H., 2003. The non-cyclooxygenase targets of non-steroidal anti-inflammatory drugs, lipoxygenases, peroxisome proliferator-activated receptor, inhibitor of κB kinase, and NF κB, do not reduce amyloid ß42 production. J. Biol. Chem. 278, 31825-31830.

Selkoe D.J., 2001. Alzheimer's disease: genes, proteins, and therapy. Physiol. Rev. 81, 741-766.

Soto, C., Kindy, M.S., Baumann, M., Frangione, B., 1996. Inhibition of Alzheimer's amyloidosis by peptides that prevent ß-sheet conformation. Biochem. Biophys. Res. Commun. 226, 672-680.

Takahashi, Y., Hayashi, I., Tominari, Y., Rikimaru, K., Morohashi. Y., Kan, T., Natsugari, H., Fukuyama, T., Tomita, T., Iwatsubo, T., 2003. Sulindac sulfide is a noncompetitive γ-secretase inhibitor that preferentially reduces Aß42 generation. J. Biol. Chem. 278, 18664-18670.

Thomas, T., Nadackal, T.G., Thomas, K., 2001. Aspirin and non-steroidal anti-inflammatory drugs inhibit amyloid-ß aggregation. NeuroReport 12, 3263-3267.

Tomiyama, T., Shoji, A., Kataoka, K., Suwa, Y., Asano, S., Kaneko, H., Endo, N., 1996. Inhibition of amyloid ß protein aggregation and neurotoxicity by rifampicin. Its possible function as a hydroxyl radical scavenger. J. Biol. Chem. 271, 6839-6844.

Weggen, S., Eriksen, J.L., Das, P., Sagi, S.A., Wang, R., Pietrzik, C.U., Findlay, K.A., Smith, T.E., Murphy, M.P., Bulter, T., Kang, D.E., Marquez-Sterling, N., Golde, T.E., Koo, E.H., 2001. A subset of NSAIDs lower amyloidogenic Aß42 independently of cyclooxygenase activity. Nature 414, 212-6.

Yang, F., Lim, G.P., Begum, A.N., Ubeda, O.J., Simmons, M.R., Ambegaokar, S.S., Chen, P.P., Kayed, R., Glabe, C.G., Frautschy, S.A., Cole, G.M., 2005. Curcumin inhibits formation of amyloid beta

oligomers and fibrils, binds plaques, and reduces amyloid in vivo. J. Biol. Chem. 280, 5892-5901.

Zeng, H., Zhang, Y., Peng, L., Shao, H., Menon, N.K., Yang, J., Salomon, A.R., Freidland, R.P., Zagorski, M.G., 2001. Nicotine and amyloid formation. Biol. Psychiatry 49, 248-257.

Zhou, Y., Su, Y., Li, B., Liu, F., Ryder, J.W., Wu, X., Gonzalez-DeWhitt, P.A., Gelfanova, V., Hale, J.E., May, P.C., Paul, S.M., Ni, B., 2003. Nonsteroidal anti-inflammatory drugs can lower amyloidogenic Aß42 by inhibiting Rho. Science 302, 1215-1217.

Legends for figures

Fig. 1. Effects of Ibu (A, B), Ket (C), and Nap (D) on the kinetics of fAß(1-40) (A, C, D) and fAß(1-42) (B) formation from fresh Aß(1-40) and Aß(1-42), respectively. The reaction mixtures containing 50 µM Aß(1-40) (A, C, D) or 25 µM Aß(1-42) (B), 50 mM phosphate buffer, pH 7.5, 100 mM NaCl, and 0 (●), 10 (○), or 50 µM (□) of Ibu (A, B), Ket (C), or Nap (D), were incubated at 37˚C for the indicated times. Each point represents the mean of three 5 µL aliquots from the same sample. Each figure is a representative pattern of 3 independent experiments.

Fig. 2. Effects of Ibu (A, B), Ket (C), and Nap (D) on the kinetics of fAß(1-40) (A, C, D) and fAß(1-42) (B) extension. The reaction mixtures containing 10 µg/mL (2.3 µM) sonicated fAß(1-40) (A, C, D) or fAß(1-42) (B), 50 µM Aß(1-40) (A, C, D) or Aß(1-42) (B), 50 mM phosphate buffer, pH 7.5, 100 mM NaCl, and 0 (●), 10 (○) or 50 µM (□) of Ibu (A, B), Ket (C), or Nap (D), were incubated at 37˚C for the indicated times. Each point represents the mean of three 5 µL aliquots from the same sample. Each figure is a representative pattern of 3 independent experiments. (E) Effect of Aß(1-40) concentration on the initial rate of fAß(1-40) extension in the presence (○) and absence (●) of Ibu. The reaction mixtures containing 10 µg/mL (2.3 µM) sonicated fAß(1-40), 50 mM phosphate buffer, pH 7.5, 100 mM NaCl, 0 (●) or 10 µM (○) Ibu, and 0, 10, 20, 30, 40, and 50 µM Aß(1-40), were incubated at 37˚C for 1 h. Points represent means of three independent experiments. In all points, standard errors were within symbols. Liner least-square fit was performed for each straight line ($R^2 = 0.971$ and 0.959 for ○ and ●, respectively).

Fig. 3. Electron micrographs of extended fAß(1-40). The reaction mixtures containing 10 µg/mL (2.3 µM) fAß(1-40), 50 µM Aß(1-40), 50 mM phosphate buffer, pH 7.5, 100 mM NaCl, and 0 (B) or 50 µM Ibu (A, C), were incubated at 37˚C for 0 (A), or 6 h (B, C). Scale bars indicate a length of 250 nm.

Fig. 4. Effects of Ibu (A,B), Ket (C), and Nap (D) on the kinetics of fAß(1-40) (A, C, D) and fAß(1-42) (B) destabilization. The reaction mixtures containing 25 µM fAß(1-40) (A, C, D) or fAß(1-42) (B), 50 mM phosphate buffer, pH 7.5, 100 mM NaCl, and 0 (●), 10 (○), or 50 µM (□) of Ibu (A, B), Ket (C), or Nap (D), were incubated at 37˚C for the indicated times. Each point represents the mean of three 5 µL aliquots from the same sample. Each figure is a representative pattern of 3 independent experiments.

Fig. 5. Electron micrographs of destabilized fAß(1-40). The reaction mixtures containing 25 µM fAß(1-40), 50 mM phosphate buffer, pH 7.5, 100 mM NaCl, and 50 µM Ibu was incubated at 37˚C for 0 (A), 1 (B), or 6 h (C). Scale bars indicate a length of 250 nm.

Fig. 6. Effects of NSAIDs on the formation of fAß(1-40) (A) and fAß(1-42) (B) from fresh Aß(1-40) and Aß(1-42), respectively, and the destabilization of fAß(1-40) (C) and fAß(1-42) (D). In (A) and (B), the reaction mixture containing 50 µM Aß(1-40) or 25 µM Aß(1-42), 50 mM phosphate buffer, pH 7.5, 100 mM NaCl, and 50 µM NSAIDs was incubated at 37˚C for 7 days and 24 h,

respectively. In (C) and (D), the reaction mixture containing 25 µM fAß(1-40) or fAß(1-42), 50 mM phosphate buffer, pH 7.5, 100 mM NaCl, and 50 µM NSAIDs was incubated at 37˚C for 24 h. Each column represents the average of three independent experiments. SD is indicated by bars. N.S. denotes not significant. Significant difference ($p < 0.05$) was observed in all other combinations (one-way analysis of variance, post-hoc test by Scheffe).

Fig. 7. Dose-dependent inhibition of the formation of fAß(1-40) (A) and fAß(1-42) (B) from fresh Aß(1-40) and Aß(1-42), respectively, and dose-dependent destabilization of fAß(1-40) (C) and fAß(1-42) (D). In (A) and (B), the reaction mixture containing 50 µM Aß(1-40) or 25 µM Aß(1-42), 50 mM phosphate buffer, pH 7.5, 100 mM NaCl, and 0, 0.01, 0.1, 1, 10 and 50 µM NDGA (●), Rif (■), SSide (□), Ibu (○), or nicotine (◆) were incubated at 37˚C for 4 days or 24 h, respectively. In (C) and (D), the reaction mixture containing 25 µM fAß(1-40) or fAß(1-42), 50 mM phosphate buffer, pH 7.5, 100 mM NaCl, and 0, 0.01, 0.1, 1, 10 and 50 µM NDGA (●), Rif (■), SSide (□), Ibu (○), or nicotine (◆) were incubated at 37˚C for 6 h. Each point represents the average of three independent experiments. SD is indicated by bars. The average without compounds was regarded as 100%. Note that the final equilibrium levels in the presence of 50 µM SSide and Ibu were different from those in Fig. 6 because different lots of Aß(1-40) and Aß(1-42) (530108 and 530914, respectively) were used in these experiments.

Fig. 8. Structures of NSAIDs examined in this study.

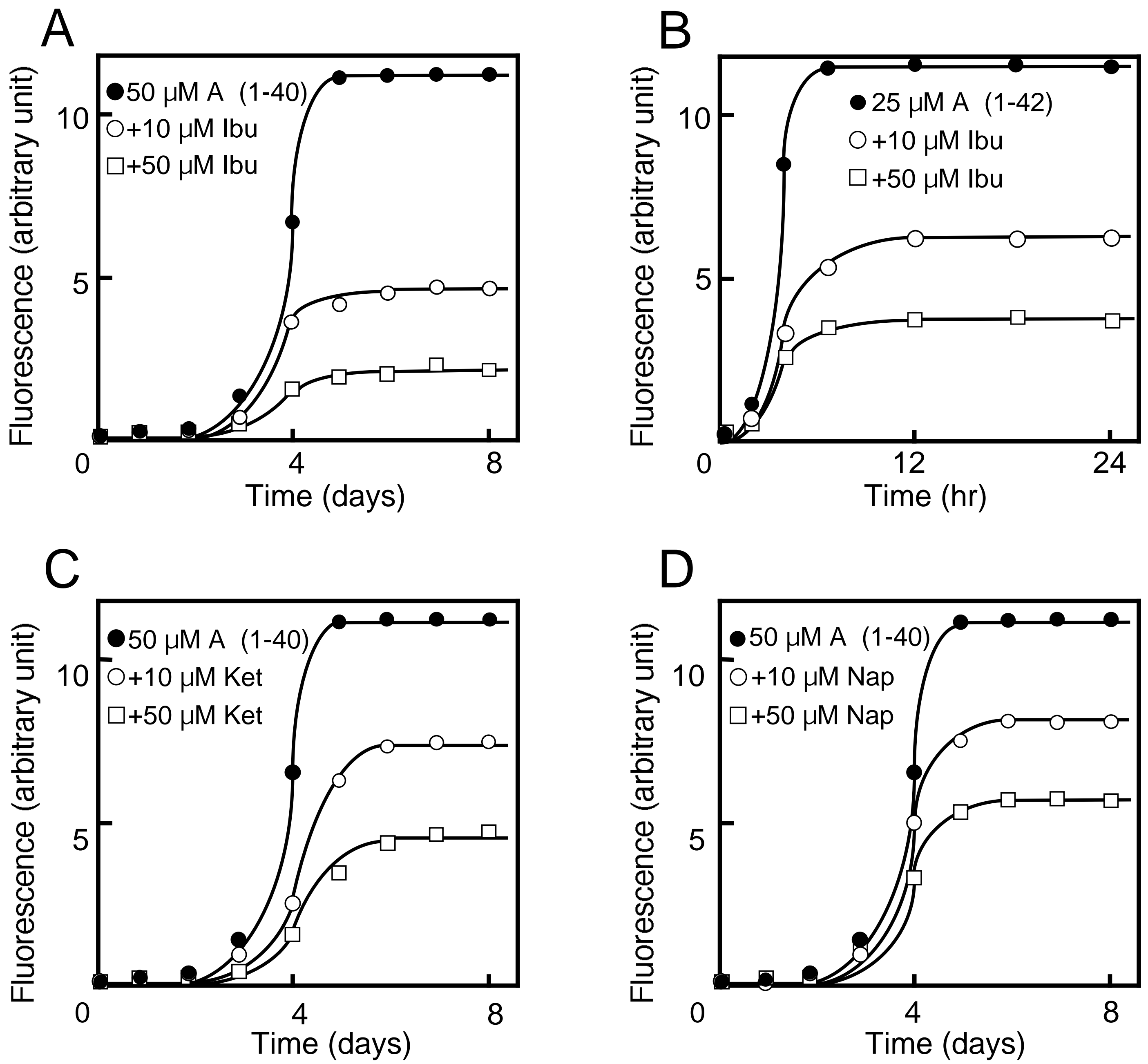

Fig. 1.

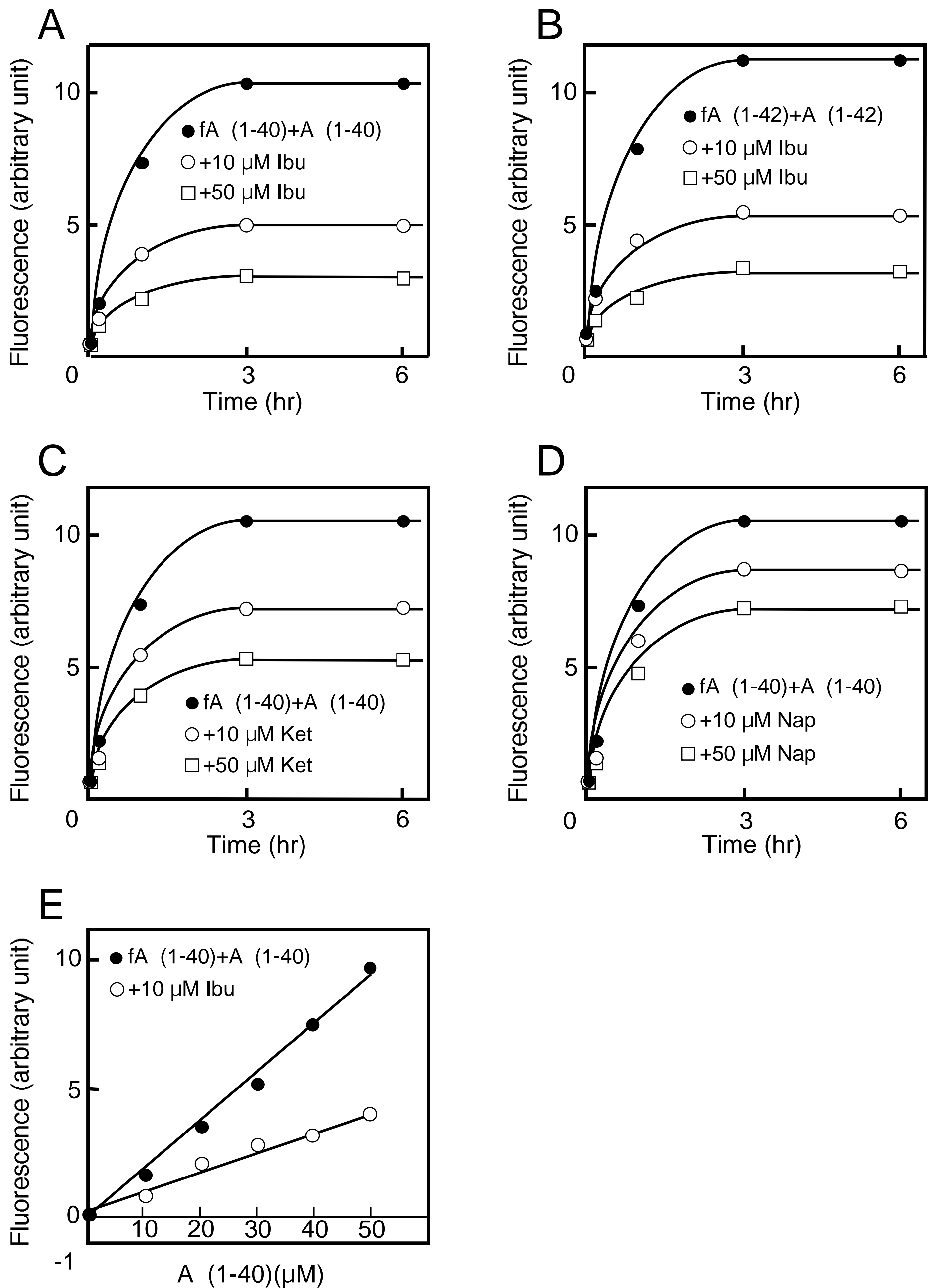

Fig. 2.

A

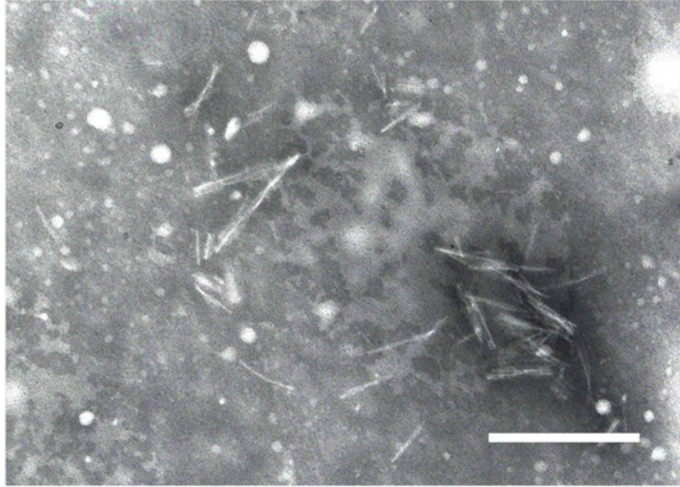

B

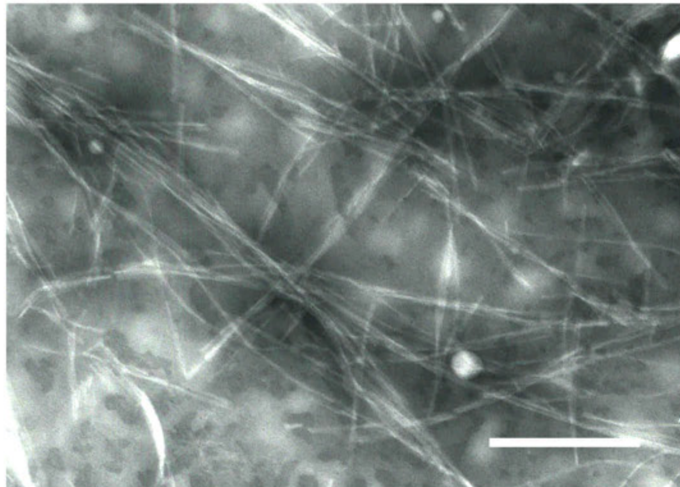

C

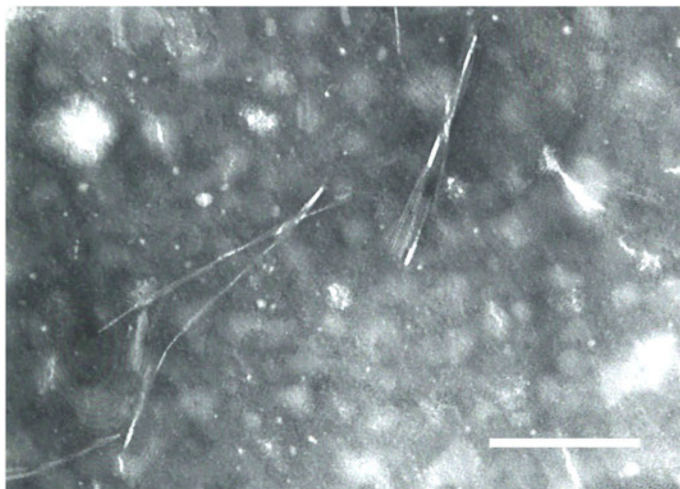

Fig. 3

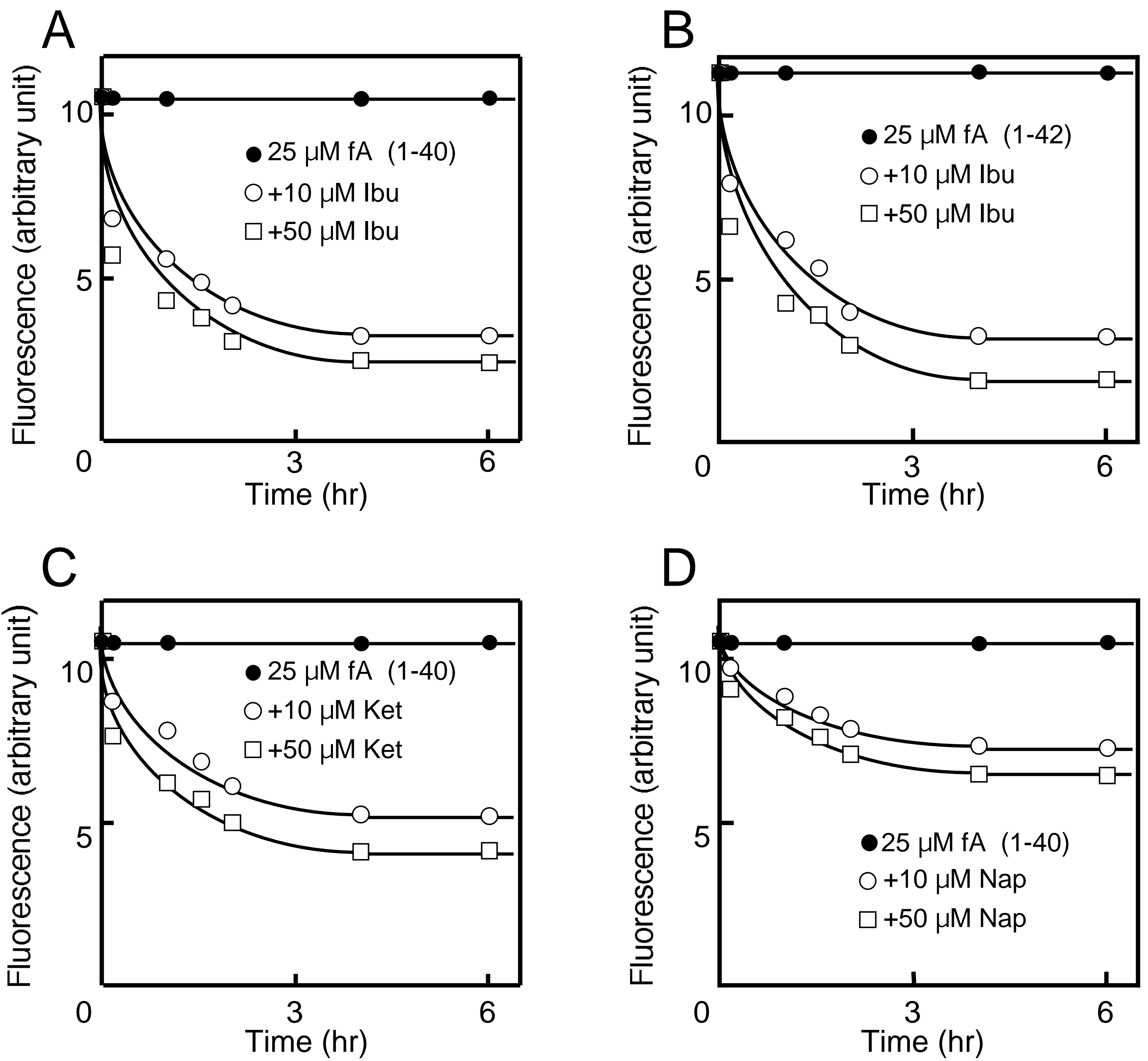

Fig. 4.

A

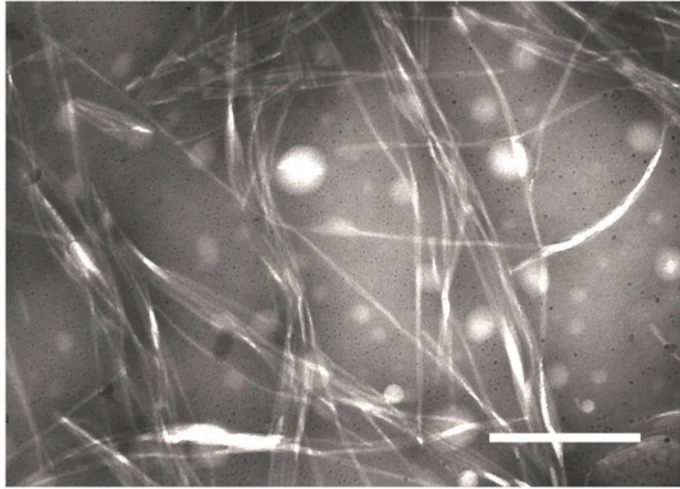

B

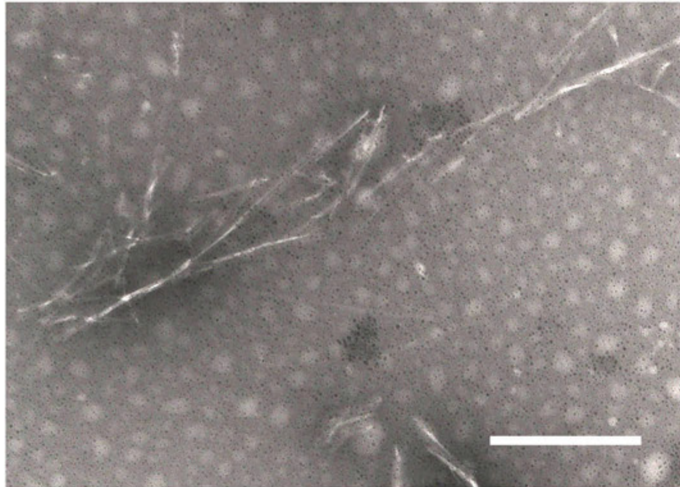

C

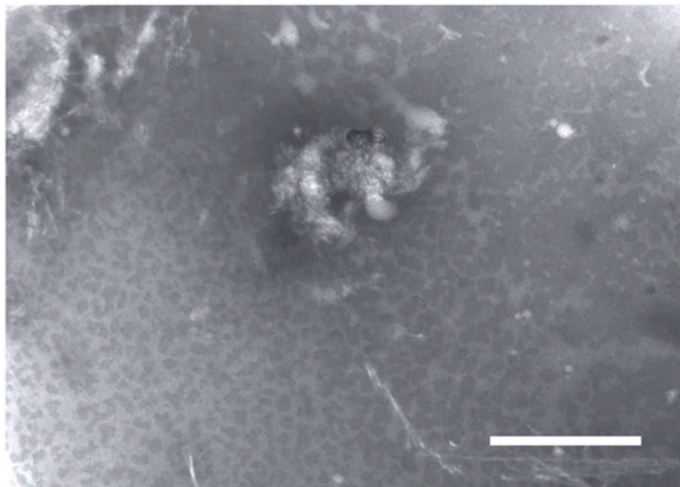

Fig. 5

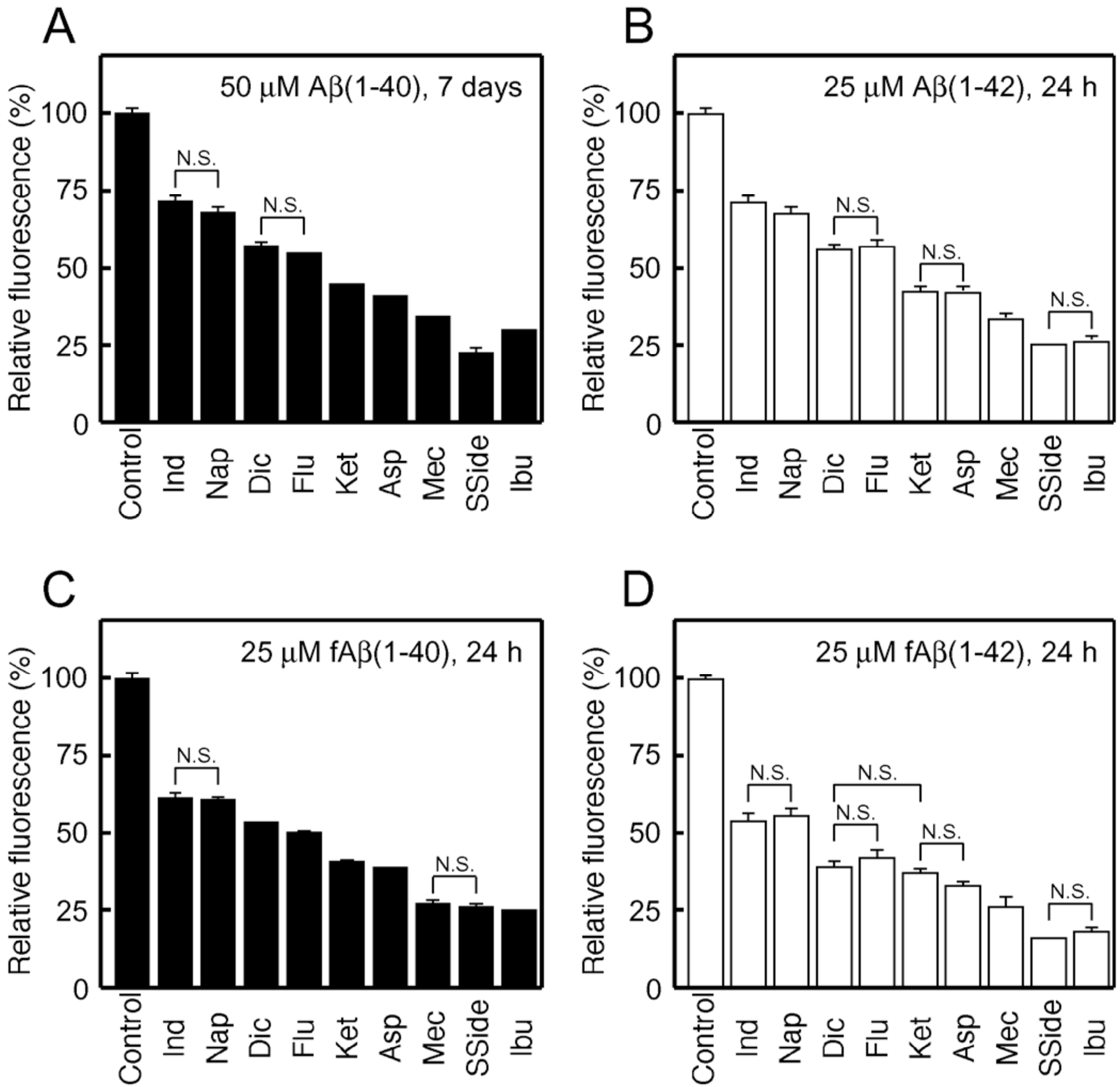

Fig. 6.

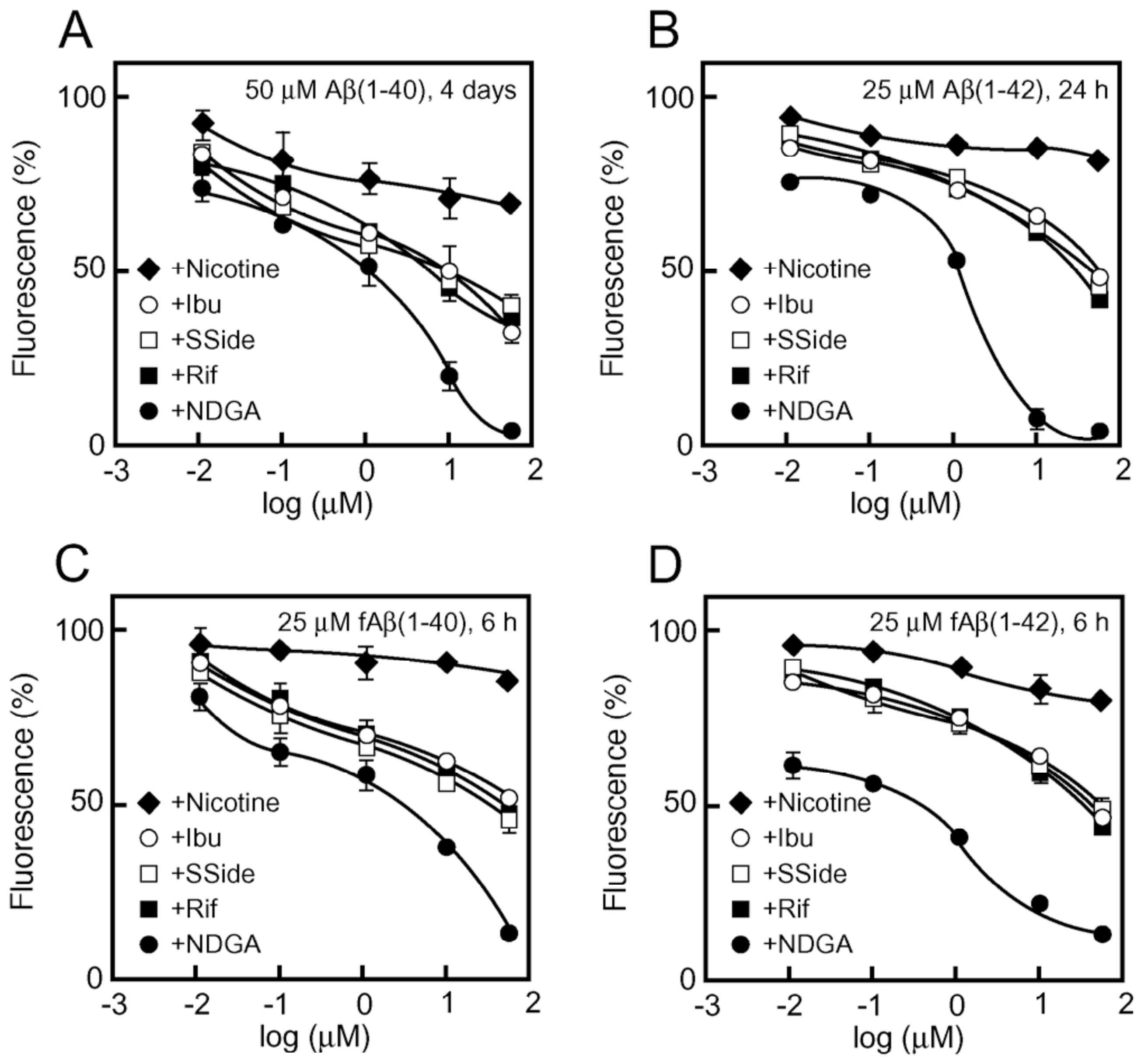

Fig. 7.

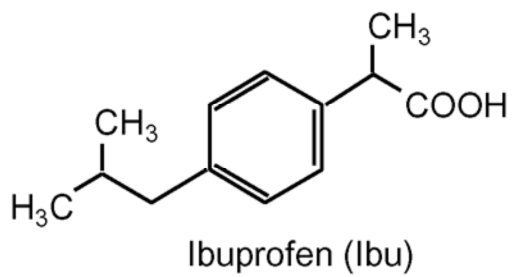

Ibuprofen (Ibu)

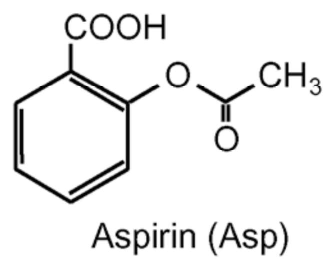

Aspirin (Asp)

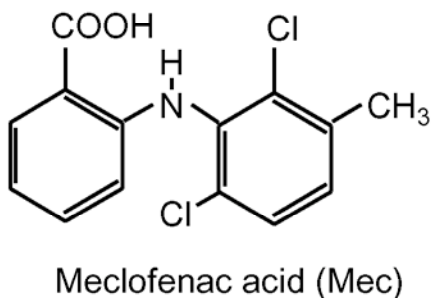

Meclofenac acid (Mec)

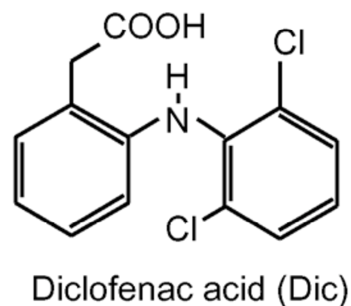

Diclofenac acid (Dic)

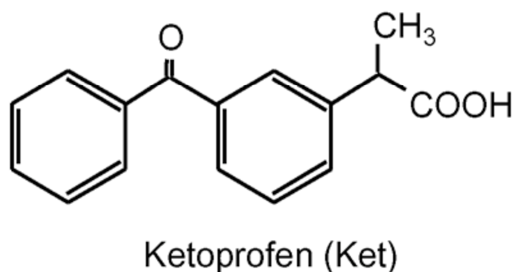

Ketoprofen (Ket)

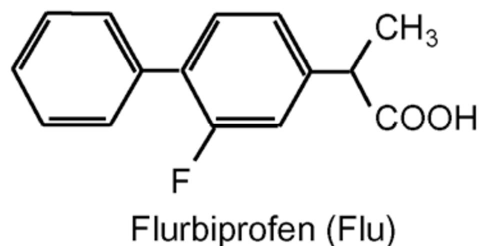

Flurbiprofen (Flu)

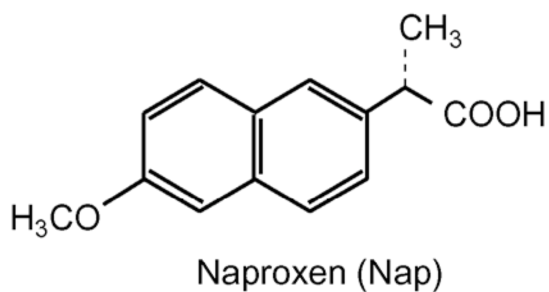

Naproxen (Nap)

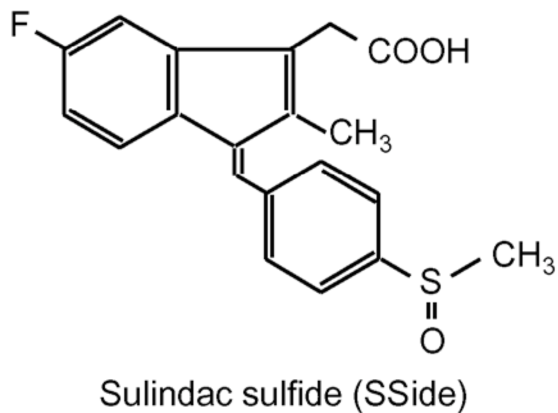

Sulindac sulfide (SSide)

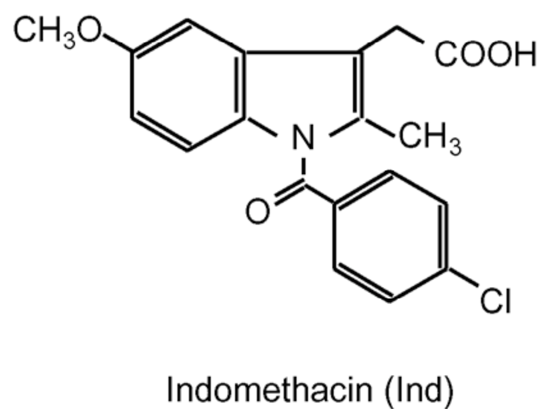

Indomethacin (Ind)

Fig. 8.